

PAPER



Cite this: *Dalton Trans.*, 2015, **44**, 4200

Received 7th October 2014,
Accepted 16th January 2015

DOI: 10.1039/c4dt03089c

www.rsc.org/dalton

Deliberate boxes and accidental wheels†

Gurpreet Kaur, Matthew I. J. Polson and Richard M. Hartshorn*

This report describes systems which combine the structural and reactive motifs of a dinucleating terpyridine-aminomethylpyridine ligand, L, with the coordination preferences and flexibilities of particular divalent metal ions to form a series of closely related box structures in a deliberate fashion. The ligand also produces unprecedented decanickel wheel complexes. Halogen to aromatic hydrogen interactions may be important in stabilising the decanickel wheel structures.

Introduction

Nature uses metal centres as both structural and reactive units in larger structural arrays.^{1–5} For example, the shapes and biological functions of zinc finger proteins and many enzymes result from a combination of the structural features of the ligands and the coordination preferences of metal ions, while the function of the photosynthetic reaction centre is intimately tied to the relative positions of the redox centres and cofactors within the protein scaffold.^{6–8} Our goal is to explore how the structural features of ligands and coordination chemistry can be used to control the assembly of polynuclear complexes containing both redox active metal ions and labile metal ions bearing exchangeable ligands.

2,2':6',2''-Terpyridine derivatives and their complexes have been extensively studied molecules since the early 20th century, due to their luminescence, spin crossover and redox properties, which have potential uses in charge storage, solar cells and photocatalysis.^{9–14} Terpyridines are excellent ligands, providing tridentate metal binding domains with high affinity for many metal ions and limited possibilities for formation of different stereoisomers.^{15–20} Thus a terpyridine ligand will bind in a meridional fashion to an octahedral metal ion and, depending on the relative amounts of metal and ligand that are present, a second ligand may bind as well.

In this paper we describe the synthesis of a terpyridine ligand that has an appended bidentate metal-binding domain and subsequent coordination chemistry in which molecular boxes have been prepared in a deliberate fashion.

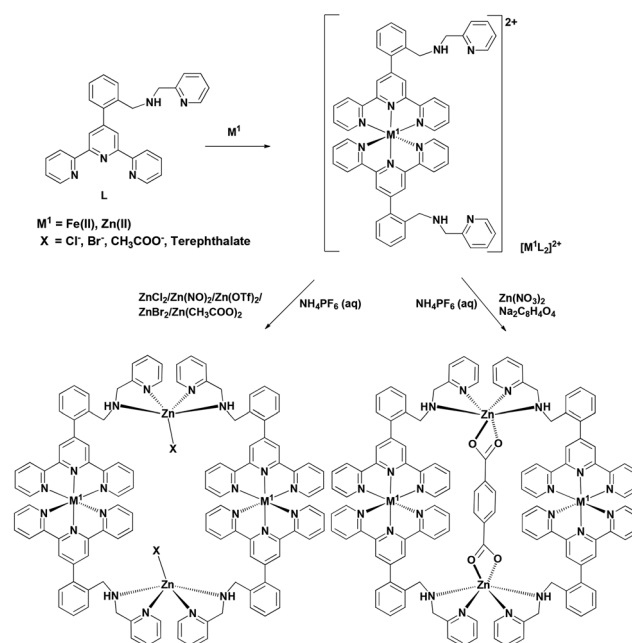
Department of Chemistry, University of Canterbury, Private Bag 4800, Christchurch 8140, New Zealand. E-mail: richard.hartshorn@canterbury.ac.nz;
Fax: +64 3 364 2110; Tel: +64 3 364 2874

† Electronic supplementary information (ESI) available: Crystallographic detail. CCDC 1011648, 1011574, 1011644, 1011645 and 1039222. For ESI and crystallographic data in CIF or other electronic format see DOI: 10.1039/c4dt03089c

Results and discussion

Ligand synthesis

The terpyridine-aminomethylpyridine ligand L (Scheme 1), was prepared by reaction of 2-aminomethylpyridine with a brominated terpyridine derivative, following an essentially standard terpyridine synthesis and a subsequent radical bromination reaction. The yields of the bromination reactions were variable, but the crude product mixture could be readily resubmitted to the reaction conditions if the bromination yield was low, and any residual 4'-(2'''-toluyl)-2,2':6',2''-terpyridine could be removed in the final chromatographic purification.



Scheme 1 Ligand L, contains tridentate and bidentate metal ion binding domains which have been used to prepare molecular boxes.

Boxes

Ligand L contains a tridentate terpyridine binding site which was designed to act either as a structural component through formation of a typical bis-terpyridine complex, or as a site at which to bind a metal ion bearing exchangeable ligands. The 2-aminomethylpyridine binding site allows binding of another metal ion, again carrying exchangeable ligands that could lead to catalytic activity, as shown in Scheme 1.

Adding a bidentate binding domain to a terpyridine scaffold results in formation of a new class of ligand in which the denticity and geometric preferences of the metal binding domains may be used to control the outcomes of synthetic reactions.^{21–24} Thus a metal ion such as Fe(II), with a strong preference for an octahedral geometry will link two terpyridine units and leave the bidentate site in each of the two ligands free for coordination to other more coordinationally flexible metal ions such as Zn(II). Such metal ions can be coordinated to the aminomethylpyridine ‘tail’ of the ligand, giving either an exposed catalytic site or a means to link two ML₂ units together through an additional metal centre with an incomplete ligand sphere.

The preparation and isolation of the FeL₂ complex is straight forward, as might be expected. Addition of Zn(II) salts to solutions of the FeL₂ complex, in the presence of [PF₆][−] ions, resulted in the formation of a [Fe₂Zn₂(L)₄Cl₂]⁶⁺ box complex (Fig. 1).

Given that the coordination chemistry of Zn(II) is notable for its variability in coordination number and geometry, we attempted to prepare similar box complexes in which both kinds of coordination site are occupied by Zn(II) ions. The resulting structure is also shown in Fig. 1, and this reveals that acetate ligands can also be bound to the Zn(II) ions in the bidentate sites.

The isolation of the [Zn₄L₄(OAc)₂]⁶⁺ box also enabled us to examine and eliminate the possibility of metal scrambling in the two [Fe₂Zn₂(L)₄X₂]⁶⁺ mixed metal systems. This possibility was discounted on the basis of the UV-vis measurements and molar absorptivity data (Fig. 2). The absorbance at 561 nm can be assigned principally to the Fe(II)-bis(terpyridine) chromophore based on literature precedent.^{25,26} Since the [Zn₄L₄(OAc)₂]⁶⁺ box complex is much more weakly coloured

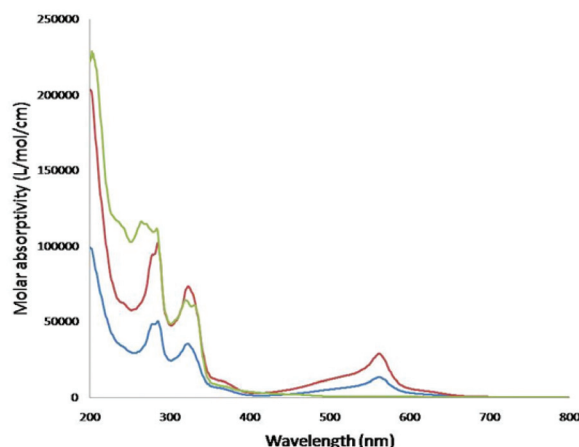


Fig. 2 UV-visible spectra of the [Fe(L)₂]²⁺ (blue) [Fe₂Zn₂(L)₄Cl₂]⁶⁺ (red) and [Zn₄(L)₄(OAc)₂]⁶⁺ (green) box complexes.

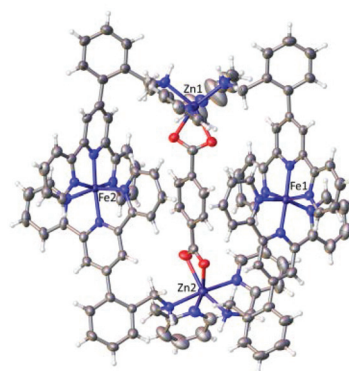


Fig. 3 The [Fe₂Zn₂(L)₄(tpt)]⁶⁺ box complex. The solvent and anions have been omitted for clarity.

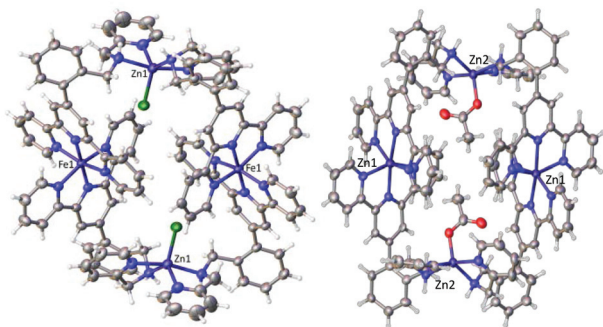


Fig. 1 The [Fe₂Zn₂(L)₄Cl₂]⁶⁺ (left) and [Zn₄L₄(OAc)₂]⁶⁺ (right) box complexes. The solvent and anions have been omitted for clarity.

($\epsilon_{561} = 670 \text{ L mol}^{-1} \text{ cm}^{-1}$) than the Fe(II)-containing boxes, and the Fe₂Zn₂L₄ complex has a molar absorptivity ($\epsilon_{561} = 28\,700 \text{ L mol}^{-1} \text{ cm}^{-1}$) slightly larger than twice the extinction coefficient of the FeL₂ complex ($\epsilon_{561} = 13\,200 \text{ L mol}^{-1} \text{ cm}^{-1}$), there must be little or no scrambling of metal ions either within or between boxes in a sample.

The bis-bidentate bridging ligand terephthalate was also deliberately encapsulated in the middle of the Fe₂Zn₂L₄ box to produce the complex where the terephthalate ion (tpt) replaces the Cl[−]/OAc[−] ligands in the coordination sphere of the Zn(II) ions (Fig. 3). Collectively, these structures invite speculation that it may be possible to bind and react molecules within these boxes.

In the solid state, each box shaped assembly is surrounded by PF₆[−] anions. In particular, two of the six PF₆[−] ions are located immediately above and below the box complexes and have two F⋯H–N hydrogen bonds to the amine groups of the box (Fig. 4). Presumably, the location of these anions helps direct the monodentate ligand on the Zn(II) centre towards the centre of the box structure.

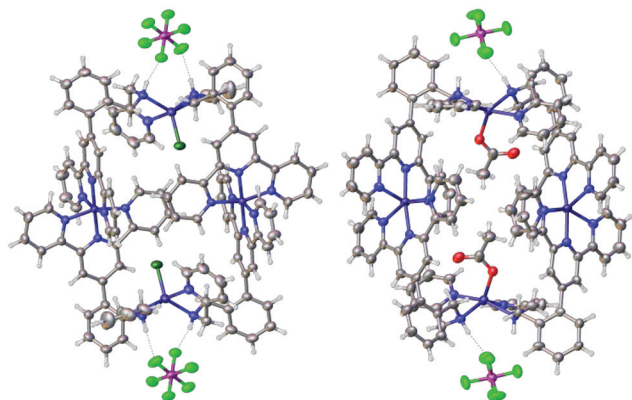


Fig. 4 Hydrogen bonding between PF_6^- ions above and below the boxes and the coordinated amine groups of the boxes. $[\text{Fe}_2\text{Zn}_2(\text{L})_4\text{Cl}_2]^{6+}$ (left) and $[\text{Zn}_4(\text{L})_4(\text{OAc})_2]^{6+}$ (right) box complexes. The solvent and spectator anions have been omitted for clarity.

Wheels

In contrast to the results from $\text{Zn}(\text{II})$ complex formation, attempts to prepare $\text{Ni}(\text{II})$ complexes of L using NiBr_2 led to isolation of the remarkable decanickel wheel complex $[\text{Ni}_{10}\text{L}_{10}\text{Br}_4(\text{H}_2\text{O})_6]^{16+}$, shown in Fig. 5, with a Br^- ion in its centre. Each six-coordinate $\text{Ni}(\text{II})$ ion is bound to the terpyridine moiety of one ligand, the aminomethylpyridine 'tail' of the terpyridine ligand bound to a neighbouring $\text{Ni}(\text{II})$ ion, and either a Br^- ion (on two of the ten $\text{Ni}(\text{II})$ ions), a water ligand (on six $\text{Ni}(\text{II})$ ions) or a disordered mixture of the two (on two $\text{Ni}(\text{II})$ ions). Thus each ligand reaches around to the next $\text{Ni}(\text{II})$ ion from the outside of the wheel, with the terpyridine units nearer to the centre of the wheel.

The wheel is approximately circular with an inner cavity diameter measured between the symmetry equivalent hydrogen atoms of 7.696 to 6.016 Å and distances between symmetry equivalent Ni of 18.933 to 20.218 Å. The outer diameter of the

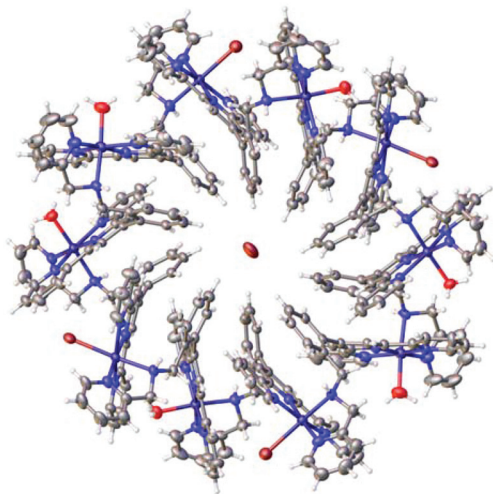


Fig. 5 $[\text{Ni}_{10}\text{L}_{10}\text{Br}_4(\text{H}_2\text{O})_6]^{16+}$ viewed down the a axis. The solvent waters, anions and ligand disorder have been omitted for clarity.

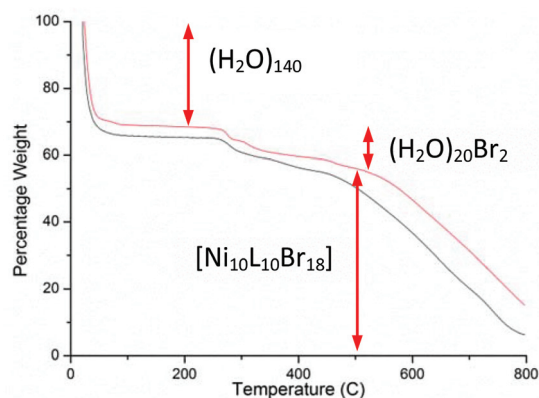


Fig. 6 Thermogravimetric analyses of the wheel complexes $[\text{Ni}_{10}\text{L}_{10}\text{Br}_4(\text{H}_2\text{O})_6]^{16+}$ (red) and $[\text{Ni}_{10}\text{L}_{10}\text{Cl}_4(\text{H}_2\text{O})_6]^{16+}$ (black).

ring varies from 29.296 to 26.515 Å and the wheel is 15.349 Å deep. The $\text{Ni}(\text{II})$ ions in the wheel are well separated from each other, both in space and through bonds.

The Br^- ion that is present inside the wheel cavity appears to be held tightly due to a number of hydrogen bonds and other atomic interactions. Fifteen uncoordinated Br^- ions are also present in the crystal lattice. The structure of the complex contains approximately 160 water molecules, randomly present in and around the wheels. These water molecules link the wheels in a 3D network by the hydrogen bond interactions between various atoms. Thermogravimetric analysis (Fig. 6) is consistent with the presence of ~ 160 water molecules, as the wheels lose approximately 30% of their mass as they are being heated to 100 °C. Samples dried in vacuum rapidly lose their crystallinity when heated through this temperature range, as do samples being heated during attempts to measure melting points.

With NiCl_2 , a similar wheel structure ($[\text{Ni}_{10}\text{L}_{10}\text{Cl}_4(\text{H}_2\text{O})_6]^{16+}$) forms (Fig. 7). Cl^- ions occupy all of the $\text{Ni}(\text{II})$ coordination sites in which Br^- ions were found in the first wheel. The remaining six $\text{Ni}(\text{II})$ ions have water ligands, as in the Br^- structure described above.

In the middle of the wheel, the smaller size of the Cl^- ion means it is disordered over two positions, each with half occupancy. This reduction in size also causes the wheel to become more elliptical, elongating to 7.748 Å along the axis of the Cl^- ion sites, and compressed to 5.686 Å in the perpendicular direction, with Ni to Ni distances of 18.880 to 20.274 Å and rim to rim distances of 29.886 to 24.551 Å. If even trace amounts of Br^- ion are present in solution, crystals are isolated in which a Br^- ion is at the centre of the wheel, while four Cl^- ions are attached to $\text{Ni}(\text{II})$ ions and another 15 are present in the lattice.

The preference for binding Br^- over Cl^- in the cavity, seems to be due to the size of the Br^- ion being the correct size to allow H-bonding with all of the ten hydrogen atoms which point into the cavity from the wheel. The off-centre distribution of the Cl^- ions over two positions within the wheel maximizes the number and strength of H-bonding interactions that the Cl^- ion can make with the wheel, given its smaller, and less optimal, size. This in turn leads to a more elliptical

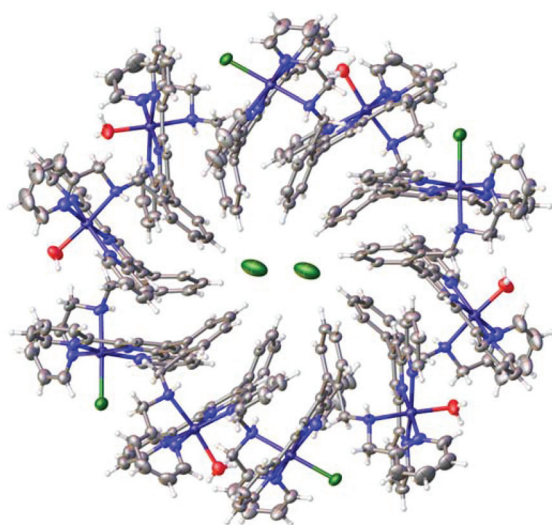


Fig. 7 $[\text{Ni}_{10}\text{L}_{10}\text{Cl}_4(\text{H}_2\text{O})_6]^{16+}$ viewed down the *a* axis. The solvent waters, anions and ligand disorder have been omitted for clarity. The two Cl^- ions shown in the centre of the structure have only half occupancy.

shape as the Cl^- wheel distorts make these H-bonds stronger. This $\text{CH}\cdots\text{X}$ tight binding of an appropriately sized central halide by multiple aromatic C–H groups has been exploited in other systems such as the triazolophane macrocycles which have been used as anion sensors.²⁷

Conclusions

A new terpyridine-aminomethylpyridine ligand has been synthesised and yields complexes in which the coordination preferences of the metal ions control the structure of the complex and provide exchangeable sites with the potential for future catalytic function. Reactions with $\text{Fe}(\text{II})$ and $\text{Zn}(\text{II})$ yield four metal centre boxes with $\text{Fe}(\text{II})$ being solely structural and $\text{Zn}(\text{II})$ ions offering coordination sites which can be occupied by different ligands without disturbing the structure. The exchangeable ligands point in towards a hydrophobic, aromatic rich environment.

When the $\text{Ni}(\text{II})$ ions bind to both sites of the ligand, an unprecedented decanuclear structure is formed. The structure has ten exchangeable sites around the wheel pointing out. A bound Br^- ion occupies the central position in the wheel in preference to an exchangeable Cl^- ion.

The $\text{F}\cdots\text{H}\cdots\text{N}$ interactions enhance the stability of the boxes and the $\text{Br}/\text{Cl}\cdots\text{C}\cdots\text{H}$ interactions play a significant role in the structures of the wheels.

Experimental

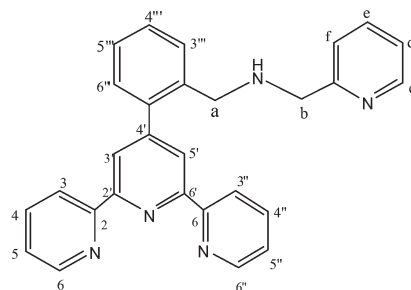
Synthesis

4'-(2'''-Toluylyl)-2,2':6',2''-terpyridine. 2-Acetylpyridine (2.4 g, 20 mmol) was added to a solution of potassium *t*-butoxide (3.36 g, 30 mmol) in freshly distilled dry THF (160 mL) and the

resultant creamy yellow suspension was treated with *o*-tolu-aldehyde (1.2 g, 10 mmol) and the mixture was stirred overnight at room temperature under nitrogen. A solution of dry ammonium acetate (15.8 g) in 2:1 ethanol–acetic acid (190 mL) was then added and the clear brown mixture obtained was heated at reflux for 5 hours. The resulting orange-yellow reaction mixture was cooled to room temperature and treated with ice (500 g) and water (2 L) to give a yellow precipitate. The precipitate was collected by filtration. Recrystallisation from ethanol gave pure 4'-(2'''-toluyl)-2,2':6',2''-terpyridine as pale yellow crystals. Yield: 2.5 g (68%); m.p. 146–152 °C; ^1H NMR (CDCl_3): δ = 8.72 (d, 2H, H_{6,6''}), 8.71 (d, 2H, H_{3,3''}), 8.49 (s, 2H, H_{3',5'}), 7.90 (t, 2H, H_{4,4''}), 7.30–7.36 (m, 6H, H_{5,5''}, toluyl), 2.38 (s, 3H, CH_3); ^{13}C NMR (CDCl_3): 156.5, 155.6, 152.2, 149.4, 139.9, 137.1, 135.4, 130.7, 129.7, 128.5, 126.2, 124.1, 121.9, 121.6, 20.7 (CH_3); ESI-MS *m/z*: $[\text{M} + \text{H}]^+$ 324.13.

4'-(2'''-(Bromomethyl)phenyl)-2,2':6',2''-terpyridine. 4'-(2'''-Toluyl)-2,2':6',2''-terpyridine (2.0 g, 6.1 mmol) and purified *N*-bromosuccinimide (1.2 g, 6.5 mmol) were added to a dry three-necked round bottom flask while flushing with N_2 . Freshly distilled CCl_4 (150 mL) was also transferred to the three-necked flask while flushing under N_2 . The solution was irradiated with a tungsten lamp for about 5 hours after adding a catalytic amount of dibenzoyl peroxide (0.002 g). The mixture was heated to 25 °C for 12 hours under N_2 . The reaction mixture was cooled to room temperature and filtered. The filtrate was concentrated under vacuum to give the crude brominated product, 4'-(2'''-(bromomethyl)phenyl)-2,2':6',2''-terpyridine as a yellow oil, which was used directly because of its tendency to decompose. Yield = 2.2 g (90%); ^1H NMR (CDCl_3) δ = 8.72 (d, 2H), 8.71 (d, 2H), 8.58 (s, 2H), 7.91 (t, 2H), 7.58 (d, 1H), 7.58 (d, 1H), 7.35–7.44 (m, 5H), 4.45 (s, 2H, CH_2Br); ^{13}C NMR (CDCl_3) 156.2, 155.8, 150.5, 149.5, 140.1, 137.3, 135.3, 131.2, 130.4, 129.2, 129.0, 124.2, 121.8, 121.7, 31.8 (CH_2Br); ESI-MS: *m/z* $[\text{M} + \text{H}]^+$ 402.0612.

4'-(2'''-(2-pyridylmethyl)aminomethyl)phenyl)-2,2':6',2''-terpyridine (L). (2-Aminomethyl)pyridine (0.53 g, 4.9 mmol) was dissolved in dry CH_3CN (100 mL), with stirring, followed by the addition of K_2CO_3 (0.68 g, 4.9 mmol). The mixture was stirred for 10 min at 35 °C. 4'-(2'''-(bromomethyl)phenyl)-2,2':6',2''-terpyridine (2.0 g, 4.9 mmol) was added to the stirring solution. The resulting mixture was heated to 50 °C for 4 days under a reflux condenser, filtered and the filtrate was taken to dryness under vacuum. The residual oil was a crude product containing L, unreacted amine and 4'-(2'''-toluyl)-2,2':6',2''-terpyridine. Yield (crude): 2.0 g (95%).



L was purified by alumina column chromatography. Initial elution with DCM removed any unreacted 4'-(2'''-toluyl)-2,2':6',2''-terpyridine. L was eluted with a 0.5% MeOH-DCM mixture. The eluate was taken to dryness and pure L was collected as a pale yellow fine powder. Yield 1.2 g (60%); m.p. 125–127 °C; Elemental analysis: Found (%): C 78.34, H 5.61, N 16.61, Calcd C₂₈H₂₃N₅ (%): C 78.44, H 5.42, N 16.34; ¹H NMR (500 MHz, CDCl₃): δ = 8.68 (d, *J* = 8, 2H, H_{3,3''}), 8.65 (d, *J* = 4, 2H, H_{6,6''}), 8.54 (s, 2H, H_{3',5'}), 8.34 (d, *J* = 5, 1H, H_c), 7.86 (td, 2H, H_{4,4''}), 7.65 (d, *J* = 8, 1H, H_{3''}), 7.42–7.38 (m, 4H, H_{5''',6''',4'',e}), 7.34 (td, 2H, H_{5,5''}), 7.23 (d, *J* = 8, 1H, H_f), 6.98 (t, *J* = 5, 1H, H_d), 3.85 (d, 4H, H_{a,b}); ¹³C NMR (500 MHz) 158.3, 156.1 (2C), 155.3 (2C), 150.9, 149.2 (2C), 149.0, 139.9, 136.8 (2C), 136.3, 135.9, 129.9–129.8 (2C), 128.7, 127.5, 123.8 (2C), 122.3, 121.9, 121.6 (2C), 121.3 (2C), 53.9, 50.5; IR (KBr, cm⁻¹) 3140 m, 3055 m, 2925 m, 2854 m, 1585 s, 1567 ssh, 1541 msh, 1466 s, 1393 w, 1335 m, 1264 m, 1131 w, 992 m, 907 w, 851 m, 762 s, 652 w, 627 m, 508 w, 467 w; ESI-MS: *m/z* [M + H⁺] 430.202, [M + 2H²⁺] 215.605, [2M + H⁺] 859.396.

[FeL₂](PF₆)₂·4H₂O. FeCl₂·2H₂O (0.05 g, 0.025 mmol) in methanol was added to a solution of L (0.02 g, 0.05 mmol) in methanol to give a purple solution, immediately. The solution was heated for 1 h while stirring and then cooled to room temperature, followed by addition of few drops of a concentrated methanolic solution of ammonium hexafluoridophosphate. An excess of cold water was also added to enhance the precipitation of complex. The purple complex was collected from the aqueous solution following centrifugation, washed with ether-methanol (2:1) solution, and dried under a N₂ stream. Yield 0.030 g, 75%; m.p. 255–260 °C; Elemental analysis Found (%): C 52.41, H 4.13, N 10.61, Calcd C₅₆H₄₆N₁₀FeP₂F₁₂·4H₂O (%): C 52.63, H 4.26, N 10.97. ¹³C NMR (CD₃CN) δ: 160.0, 157.8, 153.2, 149.8, 148.9, 138.8, 137.5, 132.1, 131.1, 130.9, 130.4, 129.7, 127.4, 124.4, 124.0, 123.3, 122.8, 51.7, 49.7; IR (KBr, cm⁻¹) 3635 s, 3064 w, 1608 m, 1573 w, 1613 m, 1545 w, 1469 m, 1423 w, 1365 m, 1288 s, 1163 w, 1056 w, 1028 w, 1000 s, 830 vs, 790 w, 754 m, 654 w, 558 s, 497 w, 458 w; ESI-MS (CH₃CN): *m/z* [Fe + 2L]²⁺ 457.1623, [Fe + 2L + PF₆ + H]²⁺ 530.1483, [Fe + 2L]²⁺ 305.1106; UV-vis (CH₃CN): λ_{max} (ε) = 275 (45 800), 287 (47 900), 322 (34 200), 561 (13 200) nm (L mol⁻¹ cm⁻¹).

[Fe₂Zn₂L₄Cl₂](PF₆)₆·4H₂O. FeCl₂·2H₂O (0.05 g, 0.025 mmol) in methanol (1 mL) was added to L (0.02 g, 0.05 mmol) in chloroform (1 mL) to give a purple solution. The resulting purple solution was treated with an excess of ZnCl₂·2H₂O in methanol. The mixture was heated for 1 h with stirring and then cooled to room temperature, followed by addition of few drops of saturated ammonium hexafluoridophosphate in methanol. An excess of cold water was added to enhance the precipitation of complex. The complex was collected by centrifugation, washed with an ether-methanol (2:1) solution, and dried under a stream of N₂. X-ray quality single crystals (fragile purple plates) were formed by slow evaporation of an acetonitrile solution. Yield 0.056 g, 60%. M.P. >280 °C. UV-vis (CH₃CN): λ_{max} (ε) = 275 (88 900), 287 (95 800), 322 (73 200), 561 (28 700), nm (L mol⁻¹ cm⁻¹). Elemental analysis found (%):

C 44.71, H 3.40, N 9.40. Calcd for C₁₁₂H₉₂N₂₀Zn₂Fe₂Cl₂P₆F₃₆·5H₂O (%): C 44.97, H 3.44, N 9.36. IR (KBr, cm⁻¹) 3340 s, 2368 w, 1844 w, 1611 m, 1535 w, 1468 w, 1368 w, 1040 w, 794 s, 626 w, 558 m, 497 w, 458 w.

[Zn₄L₄(OAc)₂](PF₆)₆·2CH₃CN. A methanolic solution of Zn(OAc)₂·2H₂O (0.01 g, 0.046 mmol) was mixed with a methanolic solution of L (0.010 g, 0.023 mmol), resulting in a pale yellow solution. The solution was then treated with a concentrated methanolic solution of ammonium hexafluoridophosphate. Later addition of an excess of cold water resulted in formation of a white precipitate. The precipitate was collected following centrifugation, and washed with methanol and ether. Vapour diffusion of di-isopropyl ether into an acetonitrile solution of the white precipitate produced colourless blocks of X-ray quality crystals within two days. Yield 0.012 g, 63%; m.p. 245–248 °C; Elemental analysis: Found (%): C 46.17, H 3.34, N 9.37, Calcd C₁₁₆H₉₈N₂₀Zn₄O₄P₆F₃₆·2H₂O (%): C 46.40, H 3.42, N 9.34; ¹H NMR (DMSO) δ = 8.86 (d, 2H), 8.83 (d, 2H), 8.69 (d, 3H), 8.23 (d, 3H), 7.85 (s, 1H), 7.67 (t, 2H), 7.54–7.46 (m, 5H), 7.17 (d, 1H), 6.98 (t, 1H), 3.80 (s, 2H), 3.76 (s, 2H); IR (KBr, cm⁻¹) 3675 w, 3340 s, 2542 w, 1866 w, 1603 s, 1575 w, 1549 w, 1478 s, 1419 w, 1371 w, 1325 w, 1248 m, 794 s, 764 w, 739 w, 658 w, 559 s, 469 w; UV-vis (CH₃CN): λ_{max} (ε) = 275 (111 200), 287 (96 800), 322 (63 400), 561 (670) nm (L mol⁻¹ cm⁻¹).

[Fe₂Zn₂L₄C₈H₄O₄](PF₆)₆. (NH₄)₂Fe(SO₄)₂·6H₂O (9 mg, 0.035 mmol) in methanol (1 mL) and L (30 mg, 0.070 mmol) in chloroform (1 mL) were mixed, producing a purple solution. Excess sodium terephthalate (70 mg) in water (5 mL) was added. After stirring for 30 min, Zn(NO₃)₂·6H₂O (20 mg, 0.070 mmol) in methanol (1 mL) was added. The mixture was heated at reflux for 8 h and then cooled to room temperature. A few drops of saturated ammonium hexafluoridophosphate in methanol and cold water (20 mL) were used to precipitate the complex. The precipitate was collected by centrifugation, washed with an ether-methanol (2:1) solution, and dried under a stream of N₂. X-ray quality single crystals (square purple plates) were formed by slow diffusion of ethyl acetate into an acetonitrile solution over a period of 3 weeks. Yield 0.056 g, 60%. M.P. >280 °C. UV-vis (CH₃CN): λ_{max} (ε) = 275 (88 300), 287 (94 830), 322 (71 800), 561 (24 720) nm (L mol⁻¹ cm⁻¹). IR (neat, cm⁻¹) 3340 s, 2368 w, 1844 w, 1698 w, 1557 s, 1551 m, 1504 w, 1381 w, 1020 w, 823 s, 789 s, 653 w, 556 m, 447 w. Elemental analysis: found (%): C 47.42, H 3.72, N 8.89. calcd for C₁₁₂H₉₂N₂₀Fe₂Zn₂C₈H₄O₄P₆F₃₆·3H₂O (%): C 47.28, H 3.37, N 9.19.

[Ni₁₀L₁₀Br₄(H₂O)₆](Br)₁₆·68H₂O. NiBr₂·3H₂O (0.008 g, 0.029 mmol) in water (10 mL) was added to L (0.006 g, 0.014 mmol) in methanol-chloroform (4:1, 5 mL), and the resulting solution was heated at reflux for 30 min. The volume of the yellow green solution of the complex was reduced to 1 mL by rotavap. The solution was filtered, and slow evaporation resulted in the formation of pale green X-ray quality crystals (blocks) over a period of 3 weeks. Yield 0.009 g, 90%. IR (KBr, cm⁻¹) 3645 w, 3190 s, 1605 s, 1550 w, 1470 m, 1417 w, 1302 w, 1247 m, 1162 w, 1055 w, 1016 s, 890 w, 772 s, 645 w,

598 w, 548 w, 516 w, 499 w, 481 w, 465 w. Elemental analysis: found (%): C 43.91, H 4.86, N 9.18%. Calcd for $C_{280}H_{230}N_{50}Ni_{10}Br_{20} \cdot 68H_2O$ (7705.19) (%): C 43.65, H 4.80, N 9.09.

X-ray crystallography

X-Ray data were collected on an Oxford-Agilent Supernova instrument with a focused microsource Cu K α [$\lambda = 1.5405 \text{ \AA}$] radiation and an ATLAS CCD area detector. CCDC 1039222, 1011648, 1011574, 1011644 and 1011645 contain the supplementary crystallographic data for this paper.

The $[Fe_2Zn_2L_4(tpt)]^{6+}$, $[Ni_{10}L_{10}Br_4(H_2O)_6]^{16+}$ and $[Ni_{10}L_{10}Cl_4(H_2O)_6]^{16+}$ structures contained significant amounts of disordered solvent molecules. This was handled systematically for the two wheel structures. First, a phase solution was found and the structure of interest was determined and refined anisotropically for all non-hydrogen atoms. Hydrogen atoms were calculated as riding atoms with thermal parameters dependant on the riding atom for all carbon atoms. For all non-carbon atoms with hydrogens except for solvent molecules, the hydrogens were located in the electron difference map, and allowed to refine at a fixed distance from the heteroatom, with a thermal parameter dependant on the riding atom. Solvent water atoms and counterions were inserted into the model as isolated, isotropic atoms where there was sufficient electron density, sufficiently distant from other solvent waters/counterions, and their occupancies were allowed to refine. This used about 60 water molecules of some occupancy in the asymmetric unit of $[Ni_{10}L_{10}Br_4(H_2O)_6]^{16+}$ and $[Ni_{10}L_{10}Cl_4(H_2O)_6]^{16+}$. Estimates of these numbers were included in the formula used for the final absorption correction, but not in the final atom count. Counterions were distinguished from solvent waters by the electron density, and were refined anisotropically. No attempt was made to model co-occupancy of a partial counterion with a solvent water. Once a stable refinement had been achieved, water molecules with an occupancy of less than one were deleted from the model and the OLEX2 solvent mask was used to correct for these poorly refined water molecules and the additional, highly disordered regions occupied by solvent water which had not been modelled. The remaining water molecules were refined as isotropic oxygen atoms, without hydrogens, due to the lack of electron density to indicate the position of the hydrogen atoms for most of the solvent waters. The total number of waters from the model and electrons corrected for in the mask (180 waters) approximately agrees with the results from TGA experiments (>160 waters).

$[Zn_4L_4(OAc)_2]^{6+}$ was solved and refined with the complex of interest, three well-ordered PF_6^- anions and one acetonitrile solvent molecule in the asymmetric unit as above. A solvent mask was used to remove a small, but poorly order void in the model (187 \AA^3).

$[Fe_2Zn_2L_4(tpt)]^{6+}$ was solved and refined with the complex of interest, four well-ordered PF_6^- anions and one acetonitrile solvent molecule in the asymmetric unit as above. The final PF_6^- anion and a single nitrate anion were poorly ordered, with the PF_6^- anion being rotationally disordered about the

phosphorus atom, occupying at least two closely spaced sites. The nitrate anion is involved in hydrogen bonding to the nitrogen atoms coordinated to the zinc atoms, and is disordered over two sites. This was modelled as disordered over two equal occupancy sites, with isotropic thermal parameters fixed at the value of the central phosphorus atom. The OLEX2 solvent mask was used to correct for the remaining unidentified solvent molecules as above. $[Fe_2Zn_2L_4Cl_2]^{6+}$ was solved and refined with the complex of interest, three independent PF_6^- anions, two half occupancy water molecules and two partial occupancy ethyl acetate molecules (0.2 and 0.3 occupancy) in the asymmetric unit. No mask was required for this structure.

Notes and references

- 1 S. Aoki and E. Kimura, *Chem. Rev.*, 2004, **104**, 769–788.
- 2 O. Waldmann, R. Koch, S. Schromm, J. Schülein, P. Müller, I. Bernt, R. W. Saalfrank, F. Hampel and E. Balthes, *Inorg. Chem.*, 2001, **40**, 2986–2995.
- 3 G. L. Abbati, A. Cornia, A. C. Fabretti, W. Malavasi, L. Schenetti, A. Caneschi and D. Gatteschi, *Inorg. Chem.*, 1997, **36**, 6443–6446.
- 4 L. Cronin, *Annu. Rep. Prog. Chem., Sect. A: Inorg. Chem.*, 2004, **100**, 323–383.
- 5 X. Lu, X. Li, Y. Cao, A. Schultz, J.-L. Wang, C. N. Moorefield, C. Wesdemiotis, S. Z. D. Cheng and G. R. Newkome, *Angew. Chem., Int. Ed.*, 2013, **52**, 7728–7731.
- 6 J. H. Laity, B. M. Lee and P. E. Wright, *Curr. Opin. Struct. Biol.*, 2001, **11**, 39–46.
- 7 S. Yamaguchi, T. Ozawa, K. Jitsukawa and H. Masuda, *Shokubai*, 2004, **46**, 299–305.
- 8 B. Jagannathan, G. Shen and J. H. Golbeck, *Adv. Photosynth. Respir.*, 2012, **33**, 285–316.
- 9 P. A. Thornley, J. C. Starkey, R. Zibaseresht, M. I. J. Polson, J. L. Wikaira and R. M. Hartshorn, *J. Coord. Chem.*, 2011, **64**, 145–158.
- 10 E. S. Bazhina, M. E. Nikiforova, G. G. Aleksandrov, N. N. Efimov, E. A. Ugolkova, V. V. Minin, S. A. Kozyukhin, A. A. Sidorov, V. M. Novotortsev and I. L. Eremenko, *Russ. Chem. Bull.*, 2012, **61**, 1084–1092.
- 11 H. El-Batal, K. Guo, X. Li, C. Wesdemiotis, C. N. Moorefield and G. R. Newkome, *Eur. J. Org. Chem.*, 2013, 3640–3644.
- 12 D. N. Chirdon, W. J. Transue, H. N. Kagalwala, A. Kaur, A. B. Maurer, T. Pintauer and S. Bernhard, *Inorg. Chem.*, 2014, **53**, 1487–1499.
- 13 G. Singh Bindra, M. Schulz, A. Paul, R. Groarke, S. Soman, J. L. Inglis, W. R. Browne, M. G. Pfeffer, S. Rau, B. J. MacLean, M. T. Pryce and J. G. Vos, *Dalton Trans.*, 2012, **41**, 13050–13059.
- 14 U. S. Schubert, H. Hofmeier and G. R. Newkome, in *Modern Terpyridine Chemistry*, Wiley-VCH Verlag GmbH & Co. KGaA, 2006, pp. 1–6, 37–38.
- 15 M. A. Bork, H. B. Vibbert, D. J. Stewart, P. E. Fanwick and D. R. McMillin, *Inorg. Chem.*, 2013, **52**, 12553–12560.

- 16 D. J. Bray, J. K. Clegg, K. A. Jolliffe, L. F. Lindoy and G. Wei, *J. Coord. Chem.*, 2008, **61**, 3–13.
- 17 G.-J. Chen, Z.-G. Wang, Y.-Y. Kou, J.-L. Tian and S.-P. Yan, *J. Inorg. Biochem.*, 2013, **122**, 49–56.
- 18 I. M. Henderson and R. C. Hayward, *Polym. Chem.*, 2012, **3**, 1221–1230.
- 19 L. Infantes, J. Chisholm and S. Motherwell, *CrystEngComm*, 2003, **5**, 480–486.
- 20 F. H. Burstall, *J. Chem. Soc.*, 1938, 1662–1672.
- 21 S. Hayami, Y. Komatsu, T. Shimizu, H. Kamihata and Y. H. Lee, *Coord. Chem. Rev.*, 2011, **255**, 1981–1990.
- 22 E. C. Constable, *Chem. Soc. Rev.*, 2007, **36**, 246–253.
- 23 R. Zibaseresht and R. M. Hartshorn, *Dalton Trans.*, 2005, 3898–3908.
- 24 M. Heller and U. S. Schubert, *Eur. J. Org. Chem.*, 2003, 947–961.
- 25 M. Chiper, M. A. R. Meier, J. M. Kranenburg and U. S. Schubert, *Macromol. Chem. Phys.*, 2007, **208**, 679–689.
- 26 E. C. Constable, D. Phillips and P. R. Raithby, *Inorg. Chem. Commun.*, 2002, **5**, 519–521.
- 27 Y. Li and A. H. Flood, *Angew. Chem., Int. Ed.*, 2008, **47**, 2649–2652.

Copyright of Dalton Transactions: An International Journal of Inorganic Chemistry is the property of Royal Society of Chemistry and its content may not be copied or emailed to multiple sites or posted to a listserv without the copyright holder's express written permission. However, users may print, download, or email articles for individual use.